Sustainable Energy & Fuels

ROYAL SOCIETY OF CHEMISTRY

PAPER

View Article Online
View Journal | View Issue

Published on 05 March 2026. Downloaded by National Institute of Technology Warangal on 4/22/2026 4:11:05 AM.

Check for updates

Cite this: *Sustainable Energy Fuels*, 2026, **10**, 1776

Transition metal chalcogenides as emerging triboelectric materials for high-performance energy harvesting devices

Gopinath M.,[ab] Rajesh Katru,[b] Navaneeth Madathil,[b] Pembarthi Raju,[b] Khanapuram Uday Kumar,*[b] Ravinder Reddy Kisannagar,[c] Inhwa Jung[c] and Rakesh Kumar Rajaboina*[b]

The search for efficient, stable, and positive triboelectric materials is urgently needed to advance triboelectric nanogenerator (TENG) technology. Addressing this gap not only enhances device performance but also supports broader sustainability objectives, aligning with SDG-driven efforts toward clean energy, innovation, and responsible material use. While progress has been made with many negative triboelectric materials, the development of their positive counterparts remains limited. Therefore, bridging this gap is essential for achieving higher efficiency TENGs. In the present work, we propose transition metal chalcogenides (TMCs), specifically vanadium tetrasulfide (VS_4), as a new tribopositive material for the first time. The positive triboelectric nature of VS_4 is experimentally verified with simple electrostatic interaction tests, surface potential values and TENG-based tests. The VS_4-based TENG achieves an open-circuit voltage of ~1.52 kV, a short-circuit current of ~180 μA, a transferred charge of ~200 nC, and a power density of 14.45 W m^{-2} under biomechanical hand-tapping force. The obtained performance is the highest among the sulphur-TMC-based TENGs reported to date. This high-performance TENG device was capable of powering a series-connected array of 720 light-emitting diodes (LEDs) and 6 LED bulbs. The present findings establish VS_4 as a new positive material for the development of triboelectric energy harvesting and self-powered systems.

Received 30th November 2025
Accepted 4th March 2026

DOI: 10.1039/d5se01579k

rsc.li/sustainable-energy

1. Introduction

The rapid advancement of self-powered systems has increased the need for efficient energy-harvesting technologies that convert ambient mechanical energy into electrical energy.[1] Since its first demonstration in 2012, the triboelectric nanogenerator (TENG) has emerged as a highly versatile and scalable energy conversion device through the synergistic effects of contact electrification and electrostatic induction.[2–4] TENGs have demonstrated remarkable capability to harvest low-frequency mechanical energy from human motion, vibrations, wind, and water waves, making them promising candidates for applications in wearable electronics, autonomous sensors, and the Internet of Things (IoT).[5–9] The overall performance of a TENG is predominantly determined by the triboelectric charge density generated during contact-separation, which strongly depends on the properties of the triboelectric materials, including their surface chemistry and roughness, effective contact area, electronic structure, dielectric constant, and ability to sustain charge trapping.[10–12] To achieve this goal, researchers across the globe have explored a wide range of organic materials, for example, polytetrafluoroethylene (PTFE), silicone elastomers, polyethylene terephthalate (PET), and Kapton, as well as inorganic materials including oxides, nitrides, 2D materials, metal organic frameworks (MOFs), MXenes, waste materials and carbon-based nanomaterials, along with their hybrid composites, to optimize triboelectric performance.[1,13–19]

Among emerging materials, transition metal chalcogenides (TMCs) have attracted attention due to their unique combination of semiconducting behavior, high mechanical flexibility, and tuneable surface properties.[17,20,21] In recent years, several TMCs, such as MoS_2, WS_2, $MoSe_2$, and WSe_2, have been successfully integrated into TENG architectures to enhance triboelectric performance and stability.[22–26] Moreover, surface engineering of TMCs and the development of TMC-polymer composites have proven effective in enhancing charge transfer, sustaining surface charge retention, and improving the output stability of triboelectric devices. For example, surface functionalization of MoS_2 with aromatic carboxylic acids alters its work function and electron affinity, leading to improved triboelectric performance and higher output power in vertical contact-mode TENGs,[25] while WS_2-based TENGs achieve higher

[a]*Department of Physics, Indian Institute of Technology (IIT) Madras, 600036, India*
[b]*Department of Physics, Energy Materials and Devices (EMD) Lab, National Institute of Technology, Warangal, 506004, India. E-mail: kanapuram.udaykumar@nitw.ac.in; rakeshr@nitw.ac.in*
[c]*Department of Mechanical Engineering, Kyung Hee University, Yongin 17104, Republic of Korea*

This journal is © The Royal Society of Chemistry 2026

Published on 05 March 2026. Downloaded by National Institute of Technology Warangal on 4/22/2026 4:11:05 AM.

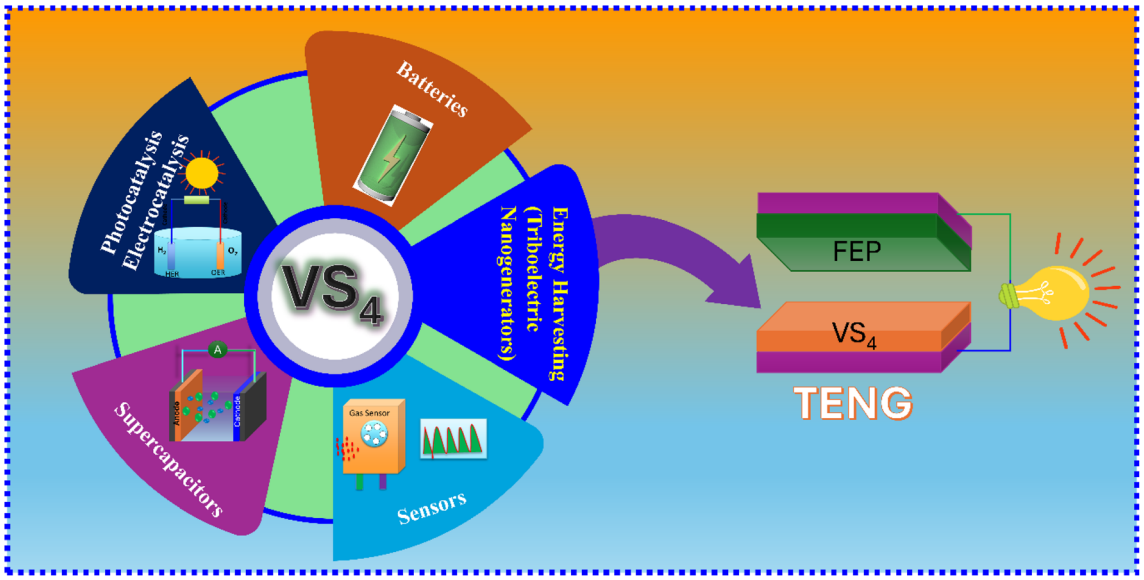

Fig. 1 Overview of VS_4 material applications in different fields with a proposed new energy harvesting application.

output voltage through thiol-ligand functionalization, which modulates surface electron affinity.[27] Bar-printed MoS_2@PVDF hybrid nanocomposite films exhibit enhanced TENG performance, reaching approximately 200 V and 11.8 μA.[28] The incorporation of MoS_2 and post annealing promotes β-phase formation and induces polarity in PVDF, improving charge storage. These wearable TENGs demonstrate excellent long-term stability and can power mobile devices and other low-power electronics. Furthermore, newly explored transition-metal carbochalcogenides (TMCCs), such as Nb_2S_2C and Ta_2S_2C, exhibit high power densities when incorporated into PDMS, highlighting the potential of layered chalcogenides for flexible triboelectric applications.[29]

Vanadium tetrasulfide (VS_4), a quasi-one-dimensional (1D) chain-like chalcogenide, has attracted increasing research interest owing to its electrochemical activity, layered structure, and high intrinsic electrical conductivity.[30] Structurally, VS_4 consists of linear chains of V^{4+} ions coordinated to disulfide (S_2^{2-}) units. These atomic chains are held together by weak van der Waals interactions, resulting in a loosely stacked crystal framework.[31] These distinctive features have enabled VS_4 to be explored in a variety of electrochemical and energy conversion applications, including batteries,[32,33] supercapacitors,[34] photocatalytic systems,[35] gas sensors,[36] and electrocatalytic hydrogen evolution reaction (HER).[37] The material's narrow bandgap, high charge carrier mobility, and chemical stability make it a promising multifunctional candidate for next-generation energy devices. Despite extensive research on its electrochemical and catalytic properties, VS_4 has not yet been explored for TENG applications. Fig. 1 illustrates various existing applications of VS_4, along with the proposed application of energy harvesting using TENG technology. This absence of study presents a significant research opportunity, as the material's semiconducting nature and electrical conductivity may substantially influence charge transport and retention mechanisms in TENG operation. To the best of the authors' knowledge, this is the first report on VS_4-based TENGs. Furthermore, this work directly contributes to SDG 7 (Clean Energy), SDG 9 (Industry & Innovation), and SDG 12 (Sustainable Production) by enabling a sustainable, battery-free, and efficient mechanical energy-harvesting technology.

In this work, we incorporated VS_4-coated adhesive conductive carbon tape attached to an aluminum (Al) substrate as a triboelectric layer, paired with different counter triboelectric layers in a vertical contact-mode device architecture for energy harvesting. The triboelectric nature of VS_4 is experimentally validated using different methods. The resulting device, when paired with fluorinated ethylene propylene (FEP), demonstrated an open-circuit voltage of ~1.52 kV, a short-circuit output current density of ~180 μA, and a power density of 14.45 W m^{-2}. Finally, the VS_4-FEP TENG was utilised to power a series-connected array of 720 LEDs and to generate sparks for applications such as microplasma generation, air ionisation, and electrostatic sterilisation. The future potential of VS_4 in triboelectric nanogenerators can be further explored by incorporating it into polymer matrices to improve device performance, stability, and durability.

2. Experimental

2.1 Materials

The precursor chemicals required for the synthesis of VS_4, such as ammonium metavanadate (NH_4VO_3), thioacetamide (CH_3CSNH_2), *N*-methyl-2-pyrrolidone (NMP), and ethanol (EtOH), were procured from Sisco Research Laboratories Pvt. Ltd (SRL).

2.2 Synthesis of VS_4

As shown in Fig. 2(a), VS_4 nanostructures were synthesised *via* a simple solvothermal method similar to the reported literature.[36,38–40] NH_4VO_3 and CH_3CSNH_2 served as the vanadium and sulphur precursors, respectively. For stoichiometric synthesis,

Published on 05 March 2026. Downloaded by National Institute of Technology Warangal on 4/22/2026 4:11:05 AM.

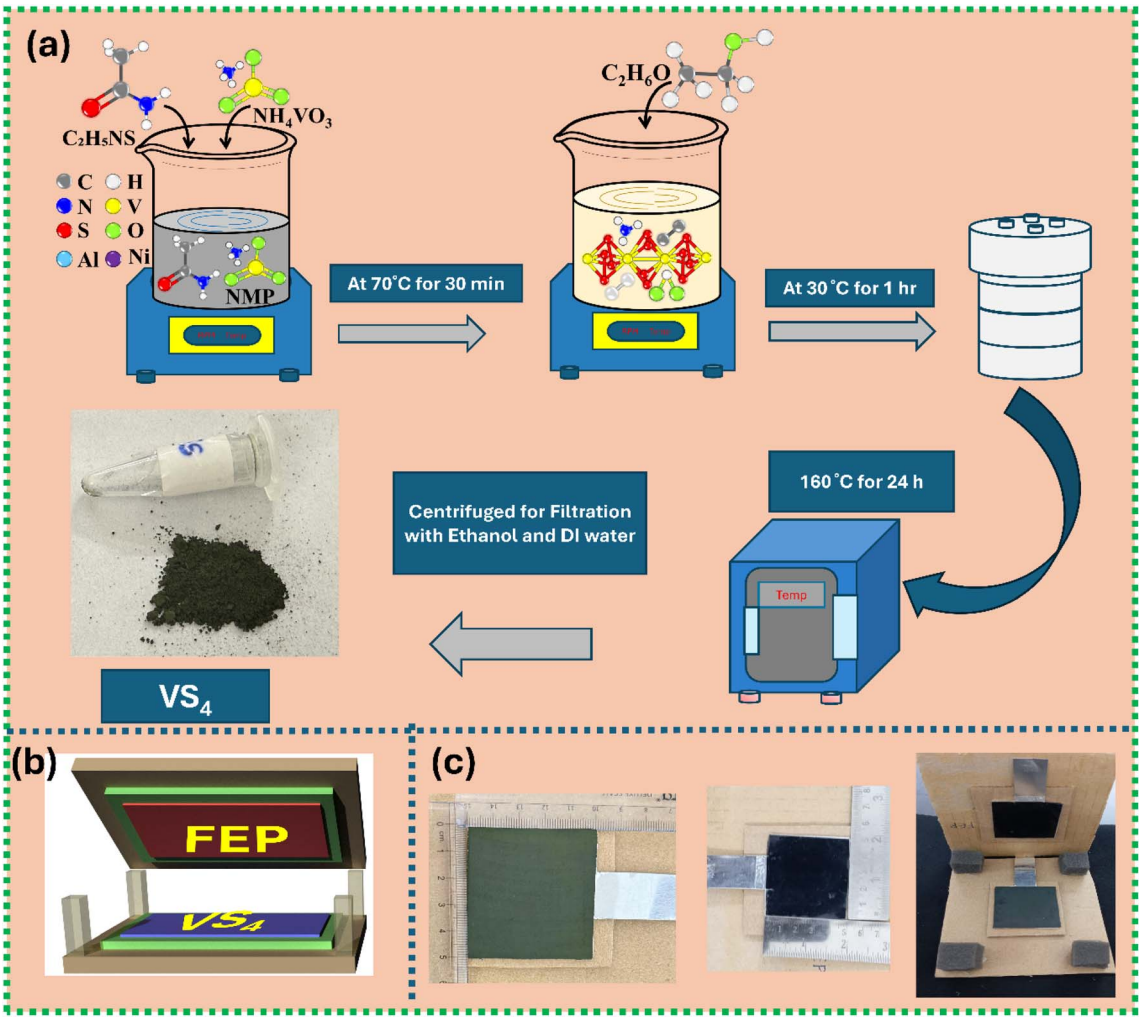

Fig. 2 (a) Synthesis procedure of VS_4 and the photograph of the obtained VS_4 powder, (b) schematic of the VS_4-FEP TENG, and (c) photographs of the frictional layers VS_4, FEP and the fabricated VS_4-FEP TENG, respectively.

0.855 mmol of NH_4VO_3 and 4 mmol of CH_3CSNH_2 were dissolved in 20 mL of *N*-methyl-2-pyrrolidone (NMP). The mixture was magnetically stirred at 70 °C for 30 minutes to ensure complete dissolution and uniform mixing of the precursors. Then, 20 mL of ethanol was added dropwise under continuous stirring at 30 °C for 1 hour. The homogeneous solution was transferred into an 80 mL Teflon-lined stainless-steel autoclave and heated at 160 °C for 24 hours. After the reaction, the autoclave was left to cool naturally to room temperature. The dark green precipitate was collected by centrifugation at 8000 rpm, and then washed multiple times with deionised water and ethanol to eliminate residual ions or organic impurities. Finally, the product was vacuum-dried at 80 °C overnight to produce VS_4 powder. Fig. 2(a) also shows the photograph of the obtained powder, which appears dark in colour.[41,42]

2.3 Formation mechanism of VS_4 nanostructures

During the solvothermal process, thioacetamide (CH_3CSNH_2) plays a dual role as both a sulfur source and a mild reducing agent. At elevated temperature, thioacetamide undergoes hydrolysis to release hydrogen sulfide (H_2S), which subsequently provides S^{2-} ions in the reaction medium. Simultaneously, NH_4VO_3 partially dissociates to yield VO_3^- and NH_4^+ ions in NMP–ethanol solution. The S^{2-} ions generated from thioacetamide gradually react with V^{5+} species from NH_4VO_3, resulting in the stepwise reduction of vanadium and the formation of intermediate vanadium oxysulfide (V–O–S) complexes. With prolonged reaction at 160 °C, these intermediates are further sulfurized to form crystalline VS_4 through anion exchange and self-assembly processes:

NMP offers strong coordination to vanadium species, preventing premature nucleation, while ethanol promotes controlled reduction and diffusion of sulfur species. The gradual nucleation and anisotropic growth under solvothermal conditions lead to the sheet/flake-like morphology. This hierarchical structure provides a large surface area and abundant active sites, which are advantageous for charge transfer and energy-harvesting applications.

2.4 Materials characterization

The obtained VS_4 powder was affixed to conductive carbon tape for morphological and compositional studies using field-

 This journal is © The Royal Society of Chemistry 2026

Published on 05 March 2026. Downloaded by National Institute of Technology Warangal on 4/22/2026 4:11:05 AM.

emission scanning electron microscopy (FESEM) (JEOL JSM-IT800). Phase identification and crystallinity were assessed by powder X-ray diffraction (PXRD) measurements, using an Anton Paar diffractometer (model: XRDYNAMIC500).

2.5 Fabrication and electrical characterization of the VS_4-TENG

A schematic of the fabricated TENG device is shown in Fig. 2(b) in vertical contact-separation mode. Initially, conductive carbon tape was affixed onto a 5 × 5 cm^2 Al substrate. On top of this tape, the synthesised VS_4 powder was uniformly coated using a soft brush. Any loosely bound powder particles were subsequently removed using air gun. The Al substrate coated with VS_4 served as the triboelectric positive layer and was mounted onto a cardboard sheet support to minimize undesired triboelectric effects from handling. Similarly, another Al substrate of identical dimensions (5 × 5 cm^2) was covered with adhesive conductive carbon tape, upon which a fluorinated ethylene propylene (FEP) film was laminated to serve as the negative triboelectric layer. This FEP-mounted Al electrode was also attached to a separate cardboard sheet. To assemble the device, sponge spacers were positioned at the four corners of one of the support cards to maintain a uniform air gap (~1 cm) between the two frictional layers. These elastic spacers acted as restoring elements, enabling the layers to separate automatically after each contact during mechanical tapping. The photographs of the prepared frictional layers and the assembled device are shown in Fig. 2(c). A series of six TENG devices was fabricated by pairing the fixed VS_4 layer with different counter triboelectric materials to evaluate performance variations. The different counter triboelectric layers include polyethene terephthalate (PET), poly methyl methacrylate (PMMA), Kapton, polytetrafluoroethylene (PTFE), silicone rubber and fluorinated ethylene propylene (FEP).

The electrical performance of the fabricated TENGs was tested under hand-tapping-induced biomechanical excitation at a frequency of approximately 4–5 Hz under ambient laboratory conditions. The open-circuit voltage (V_{oc}) and short-circuit current (I_{sc}) were recorded using a digital storage oscilloscope (DSO) and a low-noise current pre-amplifier (Stanford Research Systems, SR-570), respectively. The transferred charge was measured using an electrometer (Keithley 6514). The surface potential of the triboelectric layers was measured using a Trek 542A electrostatic voltmeter. The load-dependent output characteristics were determined using a decade resistance box, and long-term durability was assessed using an in-house-developed linear motor setup, which was operated for over ~8500 continuous contact-separation cycles and hand-tapped for 1500 cycles.

3. Results and discussion

3.1 Characterization of VS_4

The crystal structure of the synthesized VS_4 powder was examined using X-ray diffraction (XRD) analysis, and the XRD pattern is shown in Fig. 3(a). The major diffraction peaks located at 2θ values around 15.7° and 16.8° were indexed to the (110) and (020) planes of the monoclinic phase of VS_4 (JCPDS No. 072-1294).[38,43,44] The sharp, well-defined peaks confirm the high crystallinity of the prepared VS_4 powder. The absence of impurity peaks related to vanadium oxides or sulfides (*e.g.*, V_2O_5 and VS_2) indicates the phase purity of the obtained VS_4. The surface morphology of the VS_4 powder was investigated by FESEM and is presented in Fig. 3(b) and (c) at low and high magnifications. The micrographs reveal a uniform sheet-like or flower-like architecture, consistent with the reported literature.[45] Such a hierarchical structure provides a high surface area and abundant active sites, which are advantageous for triboelectric and electrochemical energy harvesting applications. Energy-dispersive X-ray spectroscopy (EDX) analysis shown in Fig. 3(d) confirms the presence of vanadium (V) and sulfur (S) as the only constituent elements without any other impurities other than small oxygen content due to oxidation.

3.2 Energy harvesting evaluation of the VS_4-TENG

The fabricated VS_4-based TENGs were evaluated for their biomechanical energy harvesting performance. The V_{oc} and I_{sc} responses of the TENG devices are presented in Fig. 4(a) and (b). Both V_{oc} and I_{sc} of VS_4-based TENGs with different opposite frictional layers exhibit a similar trend, showing the lowest output with positive triboelectric layers (PET and PMMA) and the highest output with negative triboelectric layers (silicone rubber and FEP). This observation clearly indicates that VS_4 acts as a triboelectrically positive material, and hence, can be placed on the positive side of the triboelectric series. The maximum V_{oc} and I_{sc} of ~1524 V and ~180 μA were obtained for the VS_4-FEP TENG, which was subsequently used for further studies. Fig. 4(c) and (d) shows the switching polarity test responses of the TENG, and it confirms the electrical output generated by the TENG device and not from any noise or artefacts.[46,47] Furthermore, the transferred charge during TENG operation is presented in Fig. 4(e).

The observed triboelectric positivity of VS_4 is proposed to originate from its metallic–semiconducting character combined with sulfur-rich surface termination, which leads to an electron-deficient surface and a strong tendency to donate electrons upon contact with highly electronegative materials such as FEP. The tribo-positive nature of VS_4 primarily arises from the electron-deficient V^{4+} centers coordinated by sulfur ligands. Although no permanent redox reaction occurs during contact electrification, the intrinsic electronic structure of vanadium, reflecting its thermodynamic preference toward higher oxidation states, results in reduced surface electron density and facilitates surface electron transfer. Furthermore, the disulfide (S_2^{2-}) ligands surrounding the vanadium centers exert a strong electron-withdrawing effect, creating a hole-rich surface. This synergistic electronic environment enhances electron donation from VS_4 to tribo-negative polymers such as FEP, enabling efficient charge transfer and improved output performance in TENGs.

The triboelectric nature of the synthesized VS_4 powder was further verified through a simple electrostatic interaction

Published on 05 March 2026. Downloaded by National Institute of Technology Warangal on 4/22/2026 4:11:05 AM.

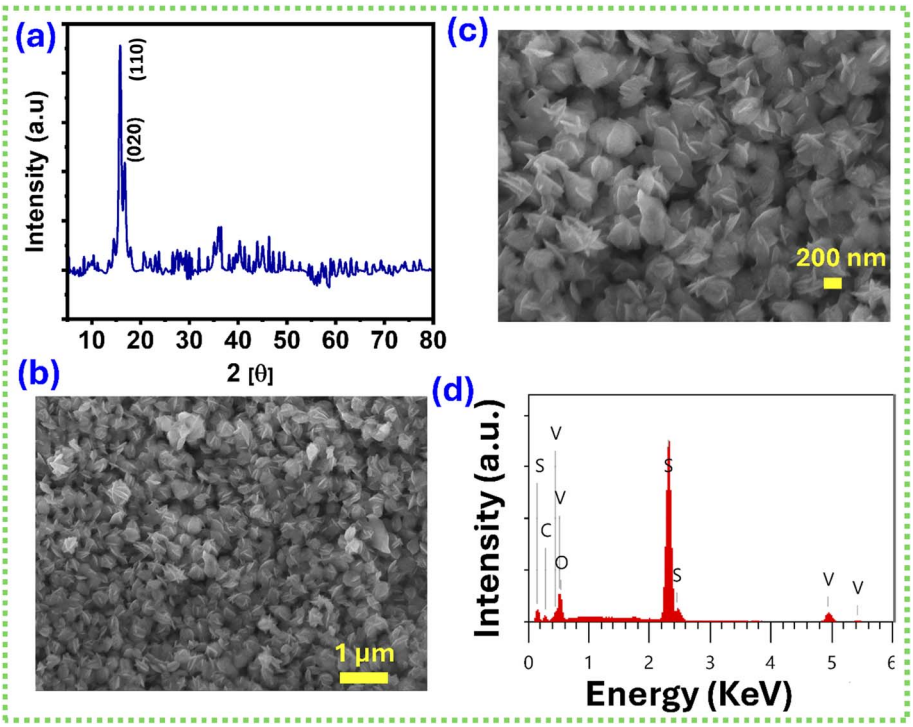

Fig. 3 (a) XRD pattern of VS_4, (b) and (c) morphology of the VS_4 powder, and (d) EDX spectrum of the VS_4 powder.

experiment. The VS_4 powder was gently spread on a plain white sheet of paper, while a Teflon rod was separately rubbed against a silk cloth to induce negative surface charges. When the negatively charged Teflon rod was brought close to the VS_4 powder, the powder particles were observed to be strongly attracted towards the Teflon surface. This clear electrostatic attraction confirms the positive triboelectric polarity of the VS_4 material. The corresponding photographs of the Teflon surface before and after interaction with VS_4 powder are presented in Fig. 4(f), and a real-time demonstration of the phenomenon is

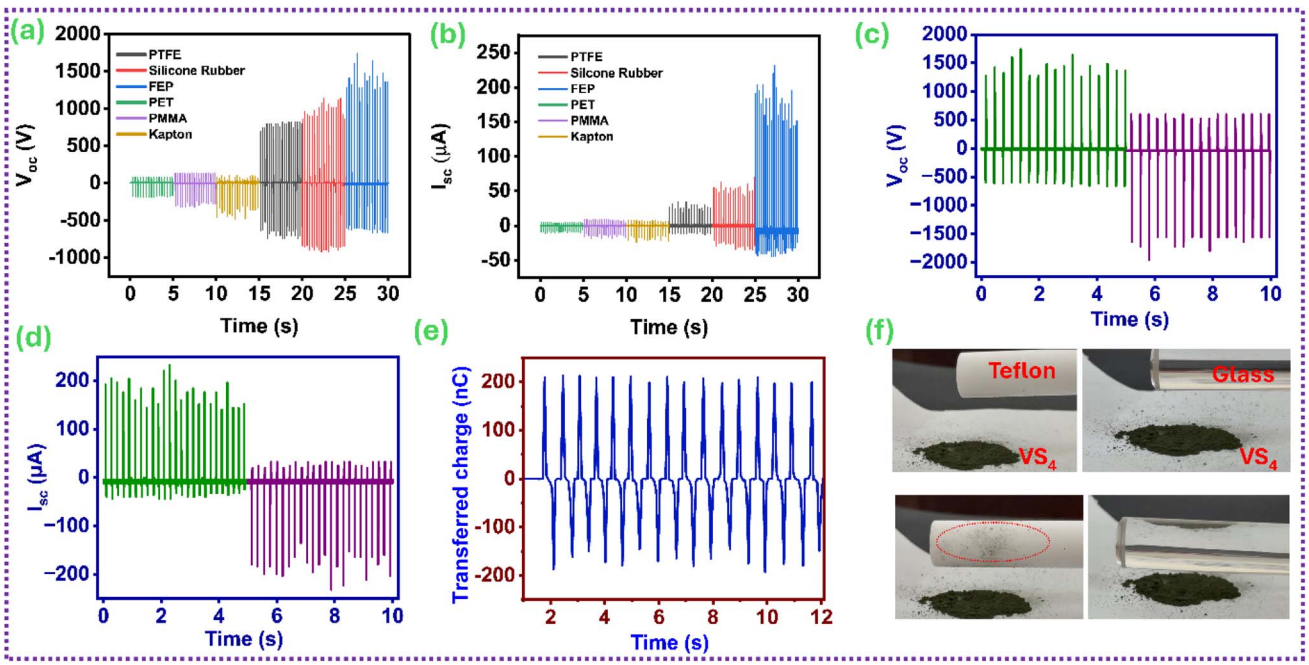

Fig. 4 Electrical output performance of VS_4-based TENGs: (a) V_{oc} and (b) I_{sc} with different opposite layers showing positive triboelectric behaviour of VS_4. (c and d) Time-dependent V_{oc} and I_{sc} of the VS_4-FEP TENG in switching polarity mode, (e) transferred charge, (f) electrostatic attraction and repulsion of VS_4 powder with a Teflon rod and a Pyrex glass rod, respectively.

 This journal is © The Royal Society of Chemistry 2026

Published on 05 March 2026. Downloaded by National Institute of Technology Warangal on 4/22/2026 4:11:05 AM.

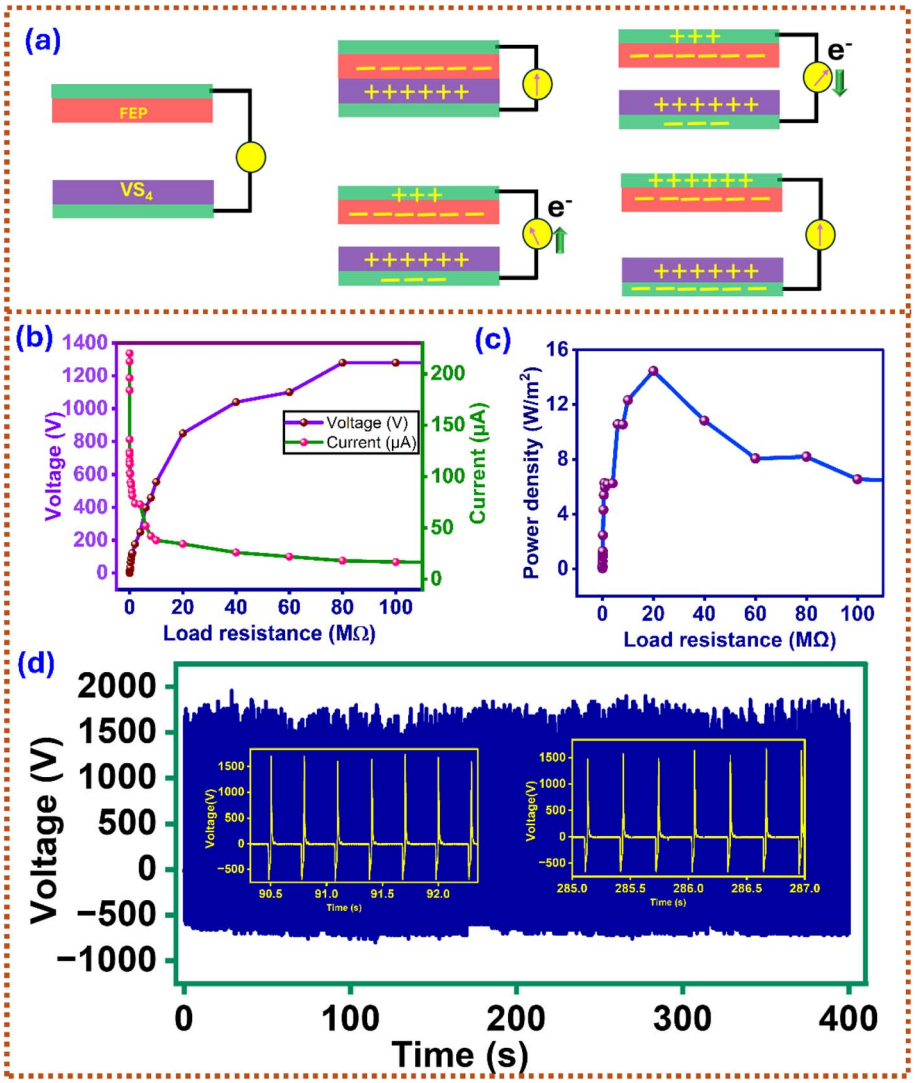

Fig. 5 (a) Working mechanism of the VS_4-FEP TENG, (b) voltage and current values of the VS_4 TENG with load resistance, (c) power density *versus* load resistance, and (d) long-term stability of the TENG over 1500 cycles (inset: magnified view of a few cycles).

provided in the SI, Video S1. In addition to this, we have also tested the electrostatic interaction of VS_4 powder with a positively charged Pyrex glass rod and found no attraction of the VS_4 particles towards the glass rod, as shown in Fig. 4(f) (SI, Video S2). This experimental verification confirms the triboelectric positive nature of VS_4. Additionally, the surface potential of a VS_4 powder film was measured after repeated contact with a FEP layer. The VS_4 film exhibited a positive surface potential of +1.17 kV, offering independent verification of its tribo-positive behavior. The real-time photograph during the testing is presented in SI Fig. S1.

Based on this confirmation of the VS_4 triboelectric positive nature, the working mechanism of the VS_4-FEP TENG is illustrated in Fig. 5(a). In the initial state (without external mechanical force), both triboelectric layers remain separated, and no charge transfer occurs across the interface, resulting in zero potential difference and no current flow in the external circuit. When a mechanical force is applied, the VS_4 and FEP layers come into intimate contact, leading to charge transfer driven by their difference in electron affinities. Owing to its lower electronegativity, VS_4 tends to lose electrons, becoming positively charged, while the FEP layer gains electrons, acquiring a net negative charge. Upon release of the applied hand-tapping force, the frictional layers separate, producing a potential difference between the electrodes that drives current through the external circuit until electrostatic equilibrium is reached. Re-application of mechanical force leads to reverse current flow in the external circuit, generating alternating current (AC) pulses with each contact-separation cycle. Hence, repetitive mechanical stimuli result in continuous AC output in the external circuit.

The load characteristics of the VS_4-based TENG were studied by varying the external load resistance from 1 kΩ to 100 MΩ, and the results are presented in Fig. 5(b). With increasing load resistance, the output voltage increased monotonically and eventually saturated at higher values, whereas the current

Published on 05 March 2026. Downloaded by National Institute of Technology Warangal on 4/22/2026 4:11:05 AM.

Table 1 Review of TENG device performances based on sulphur chalcogen-based TMC materials

Sl. no.	TMC material	Opposite frictional layer	V_{oc}	I_{sc}	Power density	Ref.
1	PVC/MoS_2 composite	PA	398 V	40 μA	1.025 W m^{-2}	49
2	MoS_2/PAN fibers	Nylon	245.3 V	5.12 μA	1.75 W m^{-2}	50
	MoS_2/PDMS		410 V	42 μA	4.52 W m^{-2}	51
	MoS_2-4,4′(oxybis)benzoic acid	Kapton	30 V	0.3 μA	399 mW m^{-2}	25
3	WS_2	PMMA	520 V	68 mA m^{-2}	0.6 W m^{-2}	23
4	WS_2	ITO	30 V	0.3 μA	40 mW m^{-2}	52
5	Cds-PDMS	Cu	236 V	17.4 μA	4 W m^{-2}	53
6	ZnS	PDMS	8 V	7.12 μA	0.43 μW m^{-2}	54
7	VS_4	FEP	1.52 kV	180 μA	14.45 W m^{-2}	Present work

decreased correspondingly due to ohmic losses. This behavior of current and voltage with load resistance is consistent with the typical load characteristics of TENGs reported in the literature.[48] The instantaneous power density ($P = V^2/R_L A$) is calculated from the voltage–load resistance data and is shown in Fig. 5(c). A maximum power density of ≈14.45 W m^{-2} under an optimal load-matching condition of 20 MΩ is observed. A comparative analysis of the VS_4-based TENG performance with previously reported TMC-based TENGs is presented in Table 1, demonstrating that the present device exhibits superior output performance in terms of voltage, current and power density.

Furthermore, the long-term operational stability of the VS_4-TENG was evaluated over 1500 consecutive hand-tapping cycles and 8500 machine-tapping cycles. Initially, the TENG was tested using an in-house-developed linear motor, with tapping for 8500 cycles; the results are shown in the SI, Fig. S2. Following the machine tapping test, the same TENG device underwent an additional 1500 hand-tapping cycles, and the results are shown in Fig. 5(d).

The device maintained remarkably stable voltage output throughout the entire test duration, indicating excellent mechanical durability and interfacial robustness of the triboelectric layers. The inset in Fig. 5(d) shows an enlarged view of several consecutive cycles, further confirming the device's reproducible and consistent performance over extended operation.

3.3 Application of the VS_4-TENG

To validate the practical energy-harvesting capability of the fabricated VS_4-based TENG, the generated electrical output was utilised to power a large array of 720 light-emitting diodes (LEDs) connected in series and mounted on multiple interconnected breadboards. Upon a single hand tap or gentle press on the VS_4-TENG, the accumulated surface charge and induced potential difference produced a high-voltage pulse sufficient to momentarily drive all LEDs simultaneously, resulting in bright and instantaneous illumination, as shown in Fig. 6(a). The real-time video demonstration of powering LEDs is presented in SI, Video S3. Similarly, a fabricated TENG can power 6 LED bulbs for a momentarily with each tap, as shown in Fig. 6(b). The real-time video demonstration of powering LED lamps is presented in SI, Video S4. These clear and uniform lighting responses indicate the TENG's ability to deliver high instantaneous current and voltage peaks, converting low-frequency

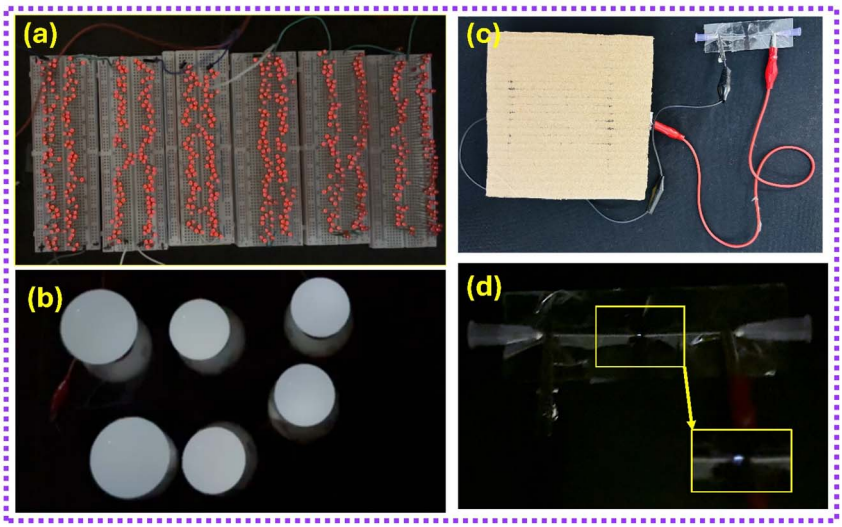

Fig. 6 (a) Photograph showing the instantaneous illumination of (a) 720 red LEDs, (b) LED lamps by the VS_4-FEP TENG upon a single hand tap, (c) experimental setup for electrical spark generation using the VS_4-FEP TENG, and (d) optical image showing a bright spark discharge between the needle tips (inset: magnified view).

 This journal is © The Royal Society of Chemistry 2026

Published on 05 March 2026. Downloaded by National Institute of Technology Warangal on 4/22/2026 4:11:05 AM.

biomechanical energy into usable electrical power without an external energy source.

Beyond energy-harvesting demonstrations, the VS_4-FEP based TENG was further evaluated for force-sensing applications by applying mechanical stimuli using different numbers of fingers (one to four). As shown in SI, Fig. S3, the output voltage increases systematically with the number of fingers: single-finger pressing produces lower voltage peaks, whereas multi-finger pressing yields progressively higher outputs. This behavior is attributed to enhanced interfacial charge generation arising from increased contact area and applied force between the friction layers. The clear, repeatable, and force-dependent electrical response confirms the high sensitivity of the VS_4-FEP TENG, highlighting its potential as a self-powered force sensor for tactile sensing,[55,56] wearable electronics,[57] and human–machine interface applications.[58]

To further demonstrate the high-voltage output capability of the fabricated VS_4-FEP based TENG, a simple spark generation experiment was carried out. The experimental step up is shown in Fig. 6(c). The output terminals of the TENG were connected to two stainless-steel needle electrodes, which were fixed on an insulating acrylic base with an adjustable air gap of approximately 1–2 mm. Upon hand tapping the TENG, the accumulated triboelectric charges on the VS_4 and FEP surfaces induced a high potential difference across the electrodes, exceeding the air breakdown voltage. As a result, a visible spark discharge was observed between the needle tips (Fig. 6(d), bottom, inset), confirming that the generated V_{oc} of the VS_4-FEP based TENG reached the kilovolt level (SI, Video S5). The observed spark confirms that the VS_4-FEP TENG can serve as a self-powered high-voltage source suitable for applications such as micro-plasma generation, air ionisation, and electrostatic sterilisation.

4. Conclusions

In summary, we have demonstrated the use of VS_4 as a new triboelectric-positive material for TENGs in efficient energy harvesting applications. The synthesised VS_4 exhibited excellent crystallinity and sheet-like morphology, enabling effective charge transfer when paired with negative triboelectric materials such as FEP. The fabricated VS_4-FEP based TENG delivered a high open-circuit voltage of ~1.52 kV, a short-circuit current of around 180 μA, and a power density of 14.45 W m^{-2}, confirming its strong capability to harvest biomechanical energy. Furthermore, the device was able to light up 720 LEDs, 6 LED bulbs and generate electrical sparks, highlighting its potential as a self-powered high-voltage source for advanced applications such as micro-plasma generation, air ionisation, and electrostatic sterilisation. This study establishes VS_4 as a promising triboelectric-positive material and suggests that other transition metal chalcogenides may also merit exploration for high-performance triboelectric nanogenerators.

Author contributions

M. Gopinath: data curation: lead; formal analysis: lead; investigation: lead; methodology: lead; writing – original draft: supporting. Rajesh Katru: data curation: supporting; formal analysis: supporting; investigation: supporting; methodology: supporting; writing – original draft: supporting. Navaneeth Madathil: data curation: supporting; formal analysis: supporting; investigation: supporting; methodology: supporting; visualization: supporting. Pembarthi Raju: data curation: supporting; formal analysis: supporting; investigation: supporting; methodology: supporting. Uday Kumar Khanapuram: conceptualization: equal; data curation: supporting; formal analysis: supporting; methodology: supporting; project administration: supporting; resources: supporting; supervision: equal; writing – review & editing: equal. Ravinder Reddy Kisannagar: data curation: supporting; formal analysis: supporting; methodology: supporting; validation: supporting; visualization: supporting; writing – original draft: supporting; writing – review & editing: supporting. Inhwa Jung: data curation: supporting formal analysis: supporting; methodology: supporting; validation: supporting; visualization: supporting; writing – review & editing: equal. Rakesh Kumar Rajaboina: conceptualization: lead; project administration: lead; resources: lead; supervision: lead; validation: lead; visualization: lead; writing – original draft: supporting; writing – review & editing: lead.

Conflicts of interest

The authors declare that they have no known competing financial interests or personal relationships that could have appeared to influence the work reported in this paper.

Data availability

The data supporting this article have been included as part of the supplementary information (SI). Supplementary information is available. See DOI: https://doi.org/10.1039/d5se01579k.

Acknowledgements

The authors R. K. R. and U. K. K. thank the Director of the National Institute of Technology – Warangal for his constant encouragement and infrastructure support. R. R. K. and K. U. K. acknowledge DAE-BRNS (59/14/06/2024-BRNS/717) for the surface potential measurement system (electrostatic voltmeter) and electrometer.

References

1 S. M. Sohel Rana, O. Faruk, M. Robiul Islam, T. Yasmin, K. Zaman and Z. L. Wang, Recent Advances in Metal-Organic Framework-Based Self-Powered Sensors: A Promising Energy Harvesting Technology, *Coord. Chem. Rev.*, 2024, **507**(16), 215741, DOI: 10.1016/j.ccr.2024.215741.
2 F. R. Fan, Z. Q. Tian and Z. Lin Wang, Flexible Triboelectric Generator, *Nano Energy*, 2012, **1**(2), 328–334, DOI: 10.1016/j.nanoen.2012.01.004.
3 W. Zhang, Y. Shi, Y. Li, X. Chen and H. Shen, A Review: Contact Electrification on Special Interfaces, *Front. Mater.*, 2022, **9**, 909746, DOI: 10.3389/fmats.2022.909746.

Published on 05 March 2026. Downloaded by National Institute of Technology Warangal on 4/22/2026 4:11:05 AM.

4 S. Pan and Z. Zhang, Fundamental Theories and Basic Principles of Triboelectric Effect: A Review, *Friction*, 2019, **7**(1), 2–17, DOI: 10.1007/s40544-018-0217-7.
5 K. Venugopal, P. Panchatcharam, A. Chandrasekhar and V. Shanmugasundaram, Comprehensive Review on Triboelectric Nanogenerator Based Wrist Pulse Measurement: Sensor Fabrication and Diagnosis of Arterial Pressure, *ACS Sens*, 2021, **6**(5), 1681–1694, DOI: 10.1021/acssensors.0c02324.
6 A. A. Mathew, A. Chandrasekhar and S. Vivekanandan, A Review on Real-Time Implantable and Wearable Health Monitoring Sensors Based on Triboelectric Nanogenerator Approach, *Nano Energy*, 2021, **80**, 105566, DOI: 10.1016/j.nanoen.2020.105566.
7 S. K. Ghosh, K. Roy, H. K. Mishra, M. R. Sahoo, B. Mahanty, P. N. Vishwakarma and D. Mandal, Rollable Magnetoelectric Energy Harvester as a Wireless IoT Sensor, *ACS Sustain. Chem. Eng.*, 2020, **8**(2), 864–873, DOI: 10.1021/acssuschemeng.9b05058.
8 S. A. Basith and A. Chandrasekhar, COVID-19 Clinical Waste Reuse: A Triboelectric Touch Sensor for IoT-Cloud Supported Smart Hand Sanitizer Dispenser, *Nano Energy*, 2023, **108**, 108183, DOI: 10.1016/j.nanoen.2023.108183.
9 P. Munirathinam and A. Chandrasekhar, Wearable Triboelectric Nanogenerator for Real-Time IoT-Supported Security Applications, *Sustain. Mater. Technol.*, 2023, **37**(4), e00700, DOI: 10.1016/j.susmat.2023.e00700.
10 X. Li, Q. Yang, D. Ren, Q. Li, H. Yang, X. Zhang and Y. Xi, A Review of Material Design for High Performance Triboelectric Nanogenerators: Performance Improvement Based on Charge Generation and Charge Loss, *Nanoscale Adv.*, 2024, **6**(18), 4522–4544, DOI: 10.1039/D4NA00340C.
11 D. Choi, Y. Lee, Z.-H. Lin, S. Cho, M. Kim, C. K. Ao, S. Soh, C. Sohn, C. K. Jeong, J. Lee, M. Lee, S. Lee, J. Ryu, P. Parashar, Y. Cho, J. Ahn, I.-D. Kim, F. Jiang, P. S. Lee, G. Khandelwal, S.-J. Kim, H. S. Kim, H.-C. Song, M. Kim, J. Nah, W. Kim, H. G. Menge, Y. T. Park, W. Xu, J. Hao, H. Park, J.-H. Lee, D.-M. Lee, S.-W. Kim, J. Y. Park, H. Zhang, Y. Zi, R. Guo, J. Cheng, Z. Yang, Y. Xie, S. Lee, J. Chung, I.-K. Oh, J.-S. Kim, T. Cheng, Q. Gao, G. Cheng, G. Gu, M. Shim, J. Jung, C. Yun, C. Zhang, G. Liu, Y. Chen, S. Kim, X. Chen, J. Hu, X. Pu, Z. H. Guo, X. Wang, J. Chen, X. Xiao, X. Xie, M. Jarin, H. Zhang, Y.-C. Lai, T. He, H. Kim, I. Park, J. Ahn, N. D. Huynh, Y. Yang, Z. L. Wang, J. M. Baik and D. Choi, Recent Advances in Triboelectric Nanogenerators: From Technological Progress to Commercial Applications, *ACS Nano*, 2023, **17**(12), 11087–11219, DOI: 10.1021/acsnano.2c12458.
12 S. M. S. Rana and Z. L. Wang, Recent Advances and Prospective Strategies for Improving the Performance of Triboelectric Nanogenerators, *Coord. Chem. Rev.*, 2025, **543**(34), 216914, DOI: 10.1016/j.ccr.2025.216914.
13 S. Potu, A. Kulandaivel, B. Gollapelli, U. K. Khanapuram and R. K. Rajaboina, Oxide Based Triboelectric Nanogenerators: Recent Advances and Future Prospects in Energy Harvesting, *Mater. Sci. Eng. R Rep.*, 2024, **161**, 100866, DOI: 10.1016/j.mser.2024.100866.
14 M. Shanbedi, H. Ardebili and A. Karim, Polymer-Based Triboelectric Nanogenerators: Materials, Characterization, and Applications, *Prog. Polym. Sci.*, 2023, **144**, 101723, DOI: 10.1016/j.progpolymsci.2023.101723.
15 S. Ghorbanzadeh and W. Zhang, Advances in MXene-Based Triboelectric Nanogenerators, *Nano Energy*, 2024, **125**, 109558, DOI: 10.1016/J.NANOEN.2024.109558.
16 K. Cheng, S. Wallaert, H. Ardebili and A. Karim, Advanced Triboelectric Nanogenerators Based on Low-Dimension Carbon Materials: A Review, *Carbon*, 2022, **194**, 81–103, DOI: 10.1016/j.carbon.2022.03.037.
17 Y. Zhou, J.-H. Zhang, S. Li, H. Qiu, Y. Shi and L. Pan, Triboelectric Nanogenerators Based on 2D Materials: From Materials and Devices to Applications, *Micromachines*, 2023, **14**(5), 1043, DOI: 10.3390/mi14051043.
18 S. K. Chittibabu, A. Chandrasekhar and K. Chintagumpala, From Energy to Intelligence: MXenes Transforming Triboelectric Nanogenerators, *J. Mater. Chem. A*, 2025, **13**(29), 23170–23226, DOI: 10.1039/d5ta02391b.
19 S. A. Basith, G. Khandelwal, D. M. Mulvihill and A. Chandrasekhar, Upcycling of Waste Materials for the Development of Triboelectric Nanogenerators and Self-Powered Applications, *Adv. Funct. Mater.*, 2024, **34**(51), 2408708, DOI: 10.1002/adfm.202408708.
20 M. Seol, S. Kim, Y. Cho, K. E. Byun, H. Kim, J. Kim, S. K. Kim, S. W. Kim, H. J. Shin and S. Park, Triboelectric Series of 2D Layered Materials, *Adv. Mater.*, 2018, **30**(39), 1–8, DOI: 10.1002/adma.201801210.
21 R. K. Rajaboina, U. K. Khanapuram and A. Kulandaivel, 2D Layered Materials Based Triboelectric Self Powered Sensors, *Adv. Sens. Res.*, 2024, **3**(10), 2400045, DOI: 10.1002/adsr.202400045.
22 M. Kim, S. H. Kim, M. U. Park, C. Lee, M. Kim, Y. Yi and K.-H. Yoo, MoS2 Triboelectric Nanogenerators Based on Depletion Layers, *Nano Energy*, 2019, **65**, 104079, DOI: 10.1016/j.nanoen.2019.104079.
23 F. Riyaz, K. P. Surendran and A. Chandran, Printed 2D WS2-Based Flexible Triboelectric Nanogenerator for Self-Powered Force and UV Sensing Applications, *Chem. Eng. J.*, 2025, **510**, 161516, DOI: 10.1016/j.cej.2025.161516.
24 V. Singh, S. Rana, R. Bokolia, A. K. Panwar, R. Meena and B. Singh, Electrospun PVDF-MoSe2 Nanofibers Based Hybrid Triboelectric Nanogenerator for Self-Powered Water Splitting System, *J. Alloys Compd.*, 2024, **978**, 173416, DOI: 10.1016/j.jallcom.2024.173416.
25 M. Biswas, D. Bhattacharya, R. Mondal, R. Bhunia, A. Garg and A. Chowdhury, Surface Engineered MoS_2 Based Novel Vertical Triboelectric Nanogenerator (VTENG) for Wireless Information Processing, *Small*, 2025, **21**(9), 241060, DOI: 10.1002/smll.202410608.
26 H. Kim, S. M. S. Rana, M. Robiul Islam, O. Faruk, K. Shrestha, G. B. Pradhan and J. Y. Park, A Molybdenum-Disulfide Nanocomposite Film-Based Stretchable Triboelectric Nanogenerator for Wearable Biomechanical Energy Harvesting and Self-Powered Human Motion Monitoring, *Chem. Eng. J.*, 2024, **491**, 151980, DOI: 10.1016/j.cej.2024.151980.

 This journal is © The Royal Society of Chemistry 2026

Published on 05 March 2026. Downloaded by National Institute of Technology Warangal on 4/22/2026 4:11:05 AM.

27 T. I. Kim, I. J. Park, S. Kang, T. S. Kim and S. Y. Choi, Enhanced Triboelectric Nanogenerator Based on Tungsten Disulfide via Thiolated Ligand Conjugation, *ACS Appl. Mater. Interfaces*, 2021, **13**(18), 21299–21309, DOI: 10.1021/acsami.1c02562.

28 B. Hedau, B. C. Kang and T. J. Ha, Enhanced Triboelectric Effects of Self-Poled MoS2-Embedded PVDF Hybrid Nanocomposite Films for Bar-Printed Wearable Triboelectric Nanogenerators, *ACS Nano*, 2022, **16**(11), 18355–18365, DOI: 10.1021/acsnano.2c06257.

29 Y. Xiao, Z. Li, D. Tan, G. Carsten and B. Xu, Triboelectric Nanogenerators Based on Transition Metal Carbo-Chalcogenide (Nb2S2C and Ta2S2C) for Energy Harvesting and Self-Powered Sensing, *Adv. Sci.*, 2024, **11**(43), e2409619, DOI: 10.1002/advs.202409619.

30 K. Yao, M. Wu, D. Chen, C. Liu, C. Xu, D. Yang, H. Yao, L. Liu, Y. Zheng and X. Rui, Vanadium Tetrasulfide for Next-Generation Rechargeable Batteries: Advances and Challenges, *Chem. Rec.*, 2022, **22**(10), e202200117, DOI: 10.1002/tcr.202200117.

31 Y. Wang, Z. Liu, C. Wang, X. Yi, R. Chen, L. Ma, Y. Hu, G. Zhu, T. Chen, Z. Tie, J. Ma, J. Liu and Z. Jin, Highly Branched VS4 Nanodendrites with 1D Atomic-Chain Structure as a Promising Cathode Material for Long-Cycling Magnesium Batteries, *Adv. Mater.*, 2018, **30**(32), e1802563, DOI: 10.1002/adma.201802563.

32 S. Wang, H. Chen, J. Liao, Q. Sun, F. Zhao, J. Luo, X. Lin, X. Niu, M. Wu, R. Li and X. Sun, Efficient Trapping and Catalytic Conversion of Polysulfides by VS4 Nanosites for Li-S Batteries, *ACS Energy Lett.*, 2019, **4**(3), 755–762, DOI: 10.1021/acsenergylett.9b00076.

33 H. Zang, F. Yang, S. Cao, M. Yang, W. Liu, F. Cai, M. Ren and Y. Wang, VS4 Nanosheets as an Excellent Anode Material for Sodium-Ion Batteries, *J. Alloys Compd.*, 2022, **899**, 163377, DOI: 10.1016/j.jallcom.2021.163377.

34 M. P. Harikrishnan and A. Chandra Bose, Recent Advances and Future Perspectives of VS_4 and Its Nanostructure Composites for Supercapacitor Applications: A Review, *Energy Fuels*, 2023, **37**(15), 10799–10826, DOI: 10.1021/acs.energyfuels.3c00866.

35 W. Guo and D. Wu, Facile Synthesis of VS4/Graphene Nanocomposites and Their Visible-Light-Driven Photocatalytic Water Splitting Activities, *Int. J. Hydrogen Energy*, 2014, **39**(30), 16832–16840, DOI: 10.1016/j.ijhydene.2014.08.088.

36 Y. Zhang, M. Yuan, X. Luo, J. Zheng, H. Su, L. Mao and Z. Chen, Ultrasensitive and Ultrafast Recovery Detection of NO2 at Room Temperature Enabled by VS4/SnS2 Hierarchical Structure, *J. Alloys Compd.*, 2025, **1039**, 183355, DOI: 10.1016/j.jallcom.2025.183355.

37 A. Karmakar, S. S. Sankar, S. Kumaravel, R. Madhu, K. H. Mahmoud, Z. M. El-Bahy and S. Kundu, Ruthenium-Doping-Induced Amorphization of VS4Nanostructures with a Rich Sulfur Vacancy for Enhanced Hydrogen Evolution Reaction in a Neutral Electrolyte Medium, *Inorg. Chem.*, 2022, **61**(3), 1685–1696, DOI: 10.1021/acs.inorgchem.1c03533.

38 W. Li, J. Huang, L. Feng, L. Cao, Y. Liu and L. Pan, VS4 Microspheres Winded by (1 1 0)-Oriented Nanotubes with High Rate Capacities as Sodium-Ion Battery Anode, *Mater. Lett.*, 2018, **230**, 105–108, DOI: 10.1016/j.matlet.2018.07.101.

39 Y. Niu, P. Luo, X. Chen, J. Song, X. He, H. Sun, Z. Li, C. Wang and J. Jiang, MXene/VS4 Self-Supporting Thin Film Electrode for Zinc-Ion Flexible Supercapacitors, *Chem. Eng. J.*, 2024, **493**, 152372, DOI: 10.1016/j.cej.2024.152372.

40 R. Katru, R. Muddamalla, K. C. Devarayapalli, H. Divi, R. K. Rajaboina, U. K. Khanapuram and D. S. Lee, VS4–NiAl LDH Composite Electrodes for next-Generation High-Performance Supercapacitors, *J. Mater. Chem. C*, 2025, **13**(31), 16024–16039, DOI: 10.1039/D5TC01244A.

41 K. Rajendran, P. Nagamony and H. Annal Therese, Template-Free Synthesis of 2D Pristine VS $_4$ Nanosheets for Supercapacitor Applications, *Phys. Status Solidi A*, 2022, **219**(19), 2200203, DOI: 10.1002/pssa.202200203.

42 G. Lui, G. Jiang, A. Duan, J. Broughton, J. Zhang, M. W. Fowler and A. Yu, Synthesis and Characterization of Template-Free VS4 Nanostructured Materials with Potential Application in Photocatalysis, *Ind. Eng. Chem. Res.*, 2015, **54**(10), 2682–2689, DOI: 10.1021/IE5042287.

43 B. Kaur, S. Naskar, P. Ghosal and M. Deepa, Suppressing Dendrite Growth with a Poly(1-Aminoanthraquinone) Coating in a VS4 Nanoflowers@carbon Nanotubes Composite Based Long Lasting Zinc-Ion Battery, *Appl. Surf. Sci.*, 2023, **610**, 155552, DOI: 10.1016/j.apsusc.2022.155552.

44 S. Li, W. He, P. Deng, J. Cui and B. Qu, Ultra-Long Cycle Life of Sodium-Ion Batteries in VS4-G Nanocomposite Structure, *Mater. Lett.*, 2017, **205**, 52–55, DOI: 10.1016/j.matlet.2017.06.058.

45 K. Rajendran, P. Nagamony and H. Annal Therese, Template-Free Synthesis of 2D-Pristine VS4 Nanosheets for Supercapacitor Applications, *Phys. Status Solidi A*, 2022, **219**(19), 2200203, DOI: 10.1002/pssa.202200203.

46 M. Jannesari, F. Ejehi, N. J. English, R. Mohammadpour, O. Akhavan and S. Shams, Triggering Triboelectric Nanogenerator Antibacterial Activities: Effect of Charge Polarity and Host Material Correlation, *Chem. Eng. J.*, 2024, **486**, 150036, DOI: 10.1016/j.cej.2024.150036.

47 N. Madathil, S. Potu, J. Pani, L. Bochu, A. Babu, H. Borkar, P. Kodali, U. K. Khanapuram and R. K. Rajaboina, Enhancing Triboelectric Nanogenerators Performance with MXene–Silicone Nanocomposites: A Leap Forward in Energy Harvesting and Touch-Sensitive Technologies, *ACS Appl. Electron. Mater.*, 2024, 5563–5574, DOI: 10.1021/acsaelm.4c00503.

48 S. Nuthalapati, A. Chakraborthy, I. Arief, K. Kumar Meena, K. Ruthvik Kaja, R. Rakesh Kumar, K. Uday Kumar, A. Das, M. Ercan Altinsoy and A. Nag, Wearable High-Performance MWCNTs/PDMS Nanocomposite-Based Triboelectric Nanogenerators for Haptic Applications, *IEEE J. Flex. Electron.*, 2024, **3**(9), 393–400, DOI: 10.1109/JFLEX.2024.3446756.

49 K. Zhao, W. Sun, X. Zhang, J. Meng, M. Zhong, L. Qiang, M.-J. Liu, B.-N. Gu, C.-C. Chung, M. Liu, F. Yu and Y.-L. Chueh, High-Performance and Long-Cycle Life of

Published on 05 March 2026. Downloaded by National Institute of Technology Warangal on 4/22/2026 4:11:05 AM.

Triboelectric Nanogenerator Using PVC/MoS2 Composite Membranes for Wind Energy Scavenging Application, *Nano Energy*, 2022, **91**, 106649, DOI: 10.1016/j.nanoen.2021.106649.

50 G. Mohana Rani, K. S. Ranjith, S. M. Ghoreishian, A. T. E. Vilian, C. Roh, R. Umapathi, Y. K. Han and Y. S. Huh, Fabrication of MoS2 Petals-Decorated PAN Fibers-Based Triboelectric Nanogenerator for Energy Harvesting and Smart Study Room Touch Sensor Applications, *Adv. Fiber Mater.*, 2024, **6**(6), 1825–1838, DOI: 10.1007/S42765-024-00453-1.

51 K. Zhao, J. Zhou, Z. Gao, J. Zhang, Y. Ye, J. Wu, Y. Ding and B. Zhang, Triboelectric Nanogenerator Fabricated from High-Charge-Density, Wear-Resistant MoS_2 Nanosheet-PDMS Composite for Energy Harvesting and Motion Detection, *ACS Appl. Electron. Mater.*, 2025, **7**(5), 1985–2000, DOI: 10.1021/acsaelm.4c02266.

52 Y.-H. Sun, W.-Z. Song, D.-J. Sun, T. Zhang, D.-S. Zhang, J. Zhang, S. Ramakrishna and Y.-Z. Long, WS2-Based Inorganic Triboelectric Nanogenerators with Light-Enhanced Output and Excellent Anti-Aging Ability, *Appl. Phys. Lett.*, 2023, **123**(15), 153901, DOI: 10.1063/5.0169224.

53 J. Mao and S. Seo, Improving the Performance of Polydimethylsiloxane-Based Triboelectric Nanogenerators by Introducing CdS Particles into the Polydimethylsiloxane Layer, *Nanomaterials*, 2023, **13**(22), 2943, DOI: 10.3390/nano13222943.

54 S. Mishra, S. Potu, R. S. Puppala, R. K. Rajaboina, P. Kodali and H. Divi, A Novel ZnS Nanosheets-Based Triboelectric Nanogenerator and Its Applications in Sensing, Self-Powered Electronics, and Digital Systems, *Mater. Today Commun.*, 2022, **31**, 103292, DOI: 10.1016/j.mtcomm.2022.103292.

55 M. Robiul Islam, O. Faruk, S. M. S. Rana, G. B. Pradhan, H. Kim, M. S. Reza, T. Bhatta and J. Y. Park, Poly-DADMAC Functionalized Polyethylene Oxide Composite Nanofibrous Mat as Highly Positive Material for Triboelectric Nanogenerators and Self-Powered Pressure Sensors, *Adv. Funct. Mater.*, 2024, **34**(40), 2403899, DOI: 10.1002/adfm.202403899.

56 R. Rameshkumar, A. Chandrasekhar and P. Selvaprabhu, Triboelectric Tactile Transducers for Neuromorphic Sensing and Synaptic Emulation: Materials, Architectures, and Interfaces, *Adv. Energy Sustain. Res.*, 2025, e202500346, DOI: 10.1002/aesr.202500346.

57 P. Pandey, K. Thapa, G. P. Ojha, M. K. Seo, K. H. Shin, S. W. Kim and J. I. Sohn, Metal-Organic Framework and Molybdenum Oxide Doped Highly Negative Hybridized Triboelectric Material for Self-Powered and Continuous Monitoring of Biosignals, *Chem. Eng. J.*, 2023, **473**, 144989, DOI: 10.1016/j.cej.2022.139209.

58 S. Zhang, S. S. Rana, T. Bhatta, G. B. Pradhan, S. Sharma, H. Song, S. Jeong and J. Y. Park, 3D Printed Smart Glove with Pyramidal MXene/Ecoflex Composite-Based Toroidal Triboelectric Nanogenerators for Wearable Human-Machine Interaction Applications, *Nano Energy*, 2023, **106**(39), 108110, DOI: 10.1016/j.nanoen.2022.108110.

 This journal is © The Royal Society of Chemistry 2026